2012

Synthesis, Characterization and Computational Study of [4]Octamethylferrocenophane

Benjamin Mark Wilson
leaftheviking2000@yahoo.com

Synthesis, Characterization and Computational Study of [4]Octamethylferrocenophane

Thesis submitted to

the Graduate College of

Marshall University

In partial fulfillment of

the requirements for the degree of

Master of Science in Chemistry

by

Benjamin Mark Wilson

Michael Castellani, Ph.D., Committee Chairperson

John Hubbard, Ph.D.

Robert Morgan, Ph.D.

Marshall University

May 2009

Abstract

Synthesis, Characterization and

Computational Study of

[4]Ferrocenophane

by Benjamin Mark Wilson

This thesis reports the synthesis of an organic molecule, 1,4-bis(2,3,4,5-tetramethylcyclopentadienyl)butane by two different methods, in about 75% and 85% crude yield. Deprotonation of this molecule followed by reaction with $FeCl_2$ generated the tethered ferrocene, [4]octamethylferrocenophane. Although the yield was low in the first attempt (2%), this molecule has been characterized through NMR spectroscopy, X-ray crystallography, electronic spectroscopy, elemental analysis, and decomposition temperature. A computational study was performed to determine the energy gap between each minimum energy structure. It was found that the energy barrier was not high enough to prevent a rapid interconversion between the two structures of minimum energy on the NMR time scale. The attempted syntheses of both 1,1'-(tetramethylene)ferrocenium tetracyanoethanide and 1,1'-(tetramethylene)cobaltocenium hexafluorophosphate are also reported although the identity of neither compound has been confirmed.

Dedication

This thesis is dedicated to my wife. Without her love and support, I could have never come this far.

I would also like to thank my mom and dad who have supported me throughout my college career.

ACKNOWLEDGMENTS

I would like to acknowledge my advisor, Dr. Castellani, for his advice and support throughout the duration of this project.

I would also like to acknowledge Drs. Price and Burcl for their help with computational chemistry.

I would like to acknowledge Drs. Anderson, O'Connor, Morgan, and Hubbard for helpful discussions.

Table of Contents

Abstract ii

Dedication iii

Acknowledgments iv

List of Figures vi

List of Tables viii

Introduction 1

Experimental Section 7

Preparation of $(C_5Me_4H)(CH_2)_4(C_5Me_4H)$ 8

Preparation of $Li_2[(C_5Me_4H)(CH_2)_4(C_5Me_4H)$ 9

Preparation of $[(C_5Me_4H)(CH_2)_4(C_5Me_4H)]Fe$ 10

Preparation of $[[(C_5Me_4H)(CH_2)_4(C_5Me_4H)]Fe][TCNE]$ 10

Preparation of $[[(C_5Me_4H)(CH_2)_4(C_5Me_4H)]Co][PF_6]$ 11

Computational Methods 11

Results and Discussion 11

Computational Results 14

Conclusions 20

Appendix 21

References 46

Lists of Figures

Figure 1: Metallocene Structure 1

Figure 2: Ferrocene in a Sigma (η^1) Configuration 1

Figures 3, 4: The Two Conformers of Ferrocene 2

Figure 5: Basic Structure of a Metallocenophane 4

Figure 6: Polymer-like Metallocenophanes 4

Figure 7: Multinuclear Metallocenophane 5

Figure 8: Ferromagnetic ordering of electron spins 5

Figure 9: Antiferromagnetic ordering of electron spins 6

Figure 10: Ferrimagnetic ordering of electron spins 6

Figure 11: Minimum Energy Structure for [4]Ferrocenophane 15

Figure 12: 1st Transition State for [4]Ferrocenophane 15

Figure 13: Intermediate Structure for [4]Ferrocenophane 16

Figure 14: Middle Transition State for [4]Ferrocenophane 16

Figure 15: The Potential Energy Curve for [4]Ferrocenophane 15

Figure 16: Minimum Energy Structure [4]Octamethylferrocenophane 16

Figure 17: 1st Transition State for [4]Octamethylferrocenophane 18

Figure 18: Intermediate Structure for [4]Octamethylferrocenophane 18

Figure 19: Middle Transition State for [4]Octamethylferrocenophane 19

Figure 20: The Potential Energy Surface for [4]Octamethylferrocenophane 19

Figures 21, 22: ^{13}C NMR Spectra of 1,4-bis(2,3,4,5-Tetramethylcyclopentadienyl)butane..... 21

Figure 23: ^{1}H NMR Spectrum of 1,4-bis(2,3,4,5-Tetramethylcyclopentadienyl)butane..... 22

Figure 24: ^{1}H NMR Spectrum of [4]Octamethylferrocenophane..... 22

Figure 25: ^{13}C NMR Spectrum of [4]Octamethylferrocenophane 23

Figure 26: X-Ray Crystal Structure of [4]Octamethylferrocenophane..... 23

Lists of Tables

Table I, II: Bond Angles for [4]Octamethylferrocenophane, ΔG for Minimum Structure 24

Table III, IV: ΔG for 1st Transition State, ΔG for Intermediate 25

Table V, VI: ΔG for the Middle Transition State, ΔG for the Minimum Structure 26

Table VII, VIII: ΔG for the 1st Transition State, ΔG for the Intermediate Structure 27

Table IX: ΔG for the Middle Transition State 28

Table X: Coordinates of the 1st Minimum Structure 29

Table XI: Coordinates of the 2nd Minimum Structure 30

Table XII: Coordinates of the 1st Transition State 31

Table XIII: Coordinates of the 2nd Transition State 32

Table XIV: Coordinates of the 1st Intermediate Structure 33

Table XV: Coordinates of the 2nd Intermediate Structure 34

Table XVI: Coordinates of the Middle Transition State 35

Table XVII: Coordinates of the 1st Minimum Structure 36

Table XVIII: Coordinates of the 2nd Minimum Structure 38

Table XIX: Coordinates of the 1st Transition State 40

Table XX: Coordinates of the 1st Intermediate Structure 42

Table XXI: Coordinates of the Middle Transition State 44

Introduction

Discovery of Metallocenes:

Metallocenes are defined as metals coordinated to two, parallel cyclopentadienyl rings (Figure 1). The first metallocene, ferrocene, was discovered serendipitously in 1951 by Kealy

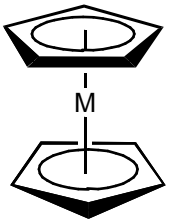

Figure 1: Metallocene Structure

and Pauson[1] who were attempting to synthesize fulvalene by using cyclopentadienyl Grignard with iron(III) chloride in a benzene/ether solvent mixture (eq 1).

$$FeCl_3 + 3\,(C_5H_5)MgBr \xrightarrow{\text{benzene/ether}} (C_5H_5)_2Fe + 1/2\,C_{10}H_{10} \quad (1)$$

Miller, Tebboth, and Tremaine[2] synthesized ferrocene before Kealy and Pauson although their paper was published at a later date. Their synthesis proceeded by passing a stream of nitrogen containing cyclopentadiene vapor over the iron to oxidize it in the presence of aluminum oxide at 300 °C (eq 2). Both groups proposed an incorrect structure in which the iron atom was only

$$Fe + Al_2O_3 + 2\,C_5H_6 \xrightarrow{300°C} (C_5H_5)_2Fe \quad (2)$$

coordinated to the cyclopentadienyl ligand in a sigma (η^1) bond configuration (Figure 2). Both

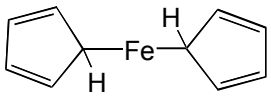

Figure 2: Ferrocene in a Sigma (η^1) Configuration

groups did note the equivalence of the carbon and hydrogen atoms in the cyclopentadienyl rings in the infrared spectrum. Their explanation was that the fluxional nature of the metal-cyclopentadienyl ligand allowed a 1,2-sigmatropic shift.[3]

In a series of communications, Wilkinson and Woodward[4,5] proposed the actual structure for $(C_5H_5)_2Fe$ and subsequent metallocenes. They considered that the proposed structure (Figure 2) did not seem reasonable because of the high stability of the product toward acids and bases. The magnetic susceptibility indicated that the molecule was diamagnetic. The infrared spectrum contained only one sharp band in the 3300-2500 cm^{-1} region which indicated that only one type of C-H bond was present. The infrared and magnetic susceptibility tests on ferrocene confirmed that the cyclopentadienyl rings should be parallel to each other with the iron atom in the middle.[4] In subsequent papers, they discussed the aromaticity of the compound and suggested the name ferrocene because of its benzene-like properties.[5] At the same time, E.O. Fischer used $(C_5H_5)Mn(CO)_3$ to demonstrate the η^5 bonding by subjecting the cyclopentadienyl ring to a Friedel-Crafts reaction.[6] X-ray crystal structures soon confirmed the predictions of Wilkinson, Woodward, and Fischer.[7]

Because the rings were determined to be parallel to each other, the rotational orientation of the rings relative to each other was questioned. Ferrocene can have two high symmetry conformers: an eclipsed structure with D_{5h} symmetry (Figure 3) or a staggered structure with D_{5d} symmetry (Figure 4).

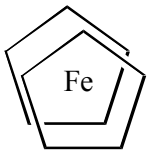

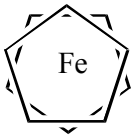

Figure 3: Ferrocene Eclipsed **Figure 4: Ferrocene Staggered**

A gas phase study of ferrocene showed that the eclipsed form is 4 kJ/mol more stable than the staggered.[8] The X-ray crystal structure, however, showed that ferrocene existed in a staggered conformation in the solid state.[7] The different structure at higher energy is a result of either intermolecular packing forces or electronic factors. Most substituted metallocenes are

more stable in the staggered conformation because of the steric interactions between the substituents.

Bonding in Ferrocene:

Bonding for the eclipsed (D_{5h}) structure of ferrocene can be explained qualitatively using two approaches, both of which yield the same result. Woodward and Rosenblum first assumed that the iron center and the cyclopentadienyl ligands were electrically neutral.[5] Using this method, each of the cyclopentadienyl ligands contributes five bonding electrons and each ring is a radical. The neutral iron atom adds 8 electrons, yielding a total of 18 electrons in the valence shell of the iron. In this model, one views the bonding as purely covalent. The other approach is to consider the cyclopentadienyl ligands as monoanions and the iron as a dication. Here each ligand would use six electrons to chelate to an iron(II) ion to make an eighteen-electron complex. An advantage of using this approach is that the cyclopentadienyl ligands are able to fulfill Hückel's rule for aromatic compounds.

Each of the cyclopentadienyl ligands combines five π molecular orbitals with the nine atomic orbitals of iron to form nineteen molecular orbitals. The highest occupied molecular orbital for ferrocene in the staggered (D_{5d}) conformation is the nonbonding a_{1g} orbital composed of the d_{z^2} and the corresponding π molecular orbital from the ligand. Similarly, the highest occupied molecular orbital for the eclipsed (D_{5h}) conformation is the a'_1 molecular orbital composed of the d_{z^2} and the corresponding π molecular orbital from the ligand.[8,9,10]

Metallocenophanes:

Metallocenes in which the cyclopentadienyl ligands are connected are called metallocenophanes. Figure 5 shows a system with a single iron atom, whereas Figures 6 and 7 show multi-metallic systems. The rings in a monometallic system may be connected by one or more tethers (Figure 5).[11] To date, several different metallocenophanes have been synthesized

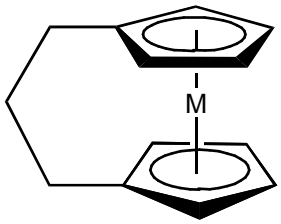

Figure 5: Metallocenophane Structure

ranging from a single dimethylene tether to having five tetramethylene tethers.[12,13] The ferrocenes containing two and three tetramethylene tethers have also been prepared.[14] One interesting fact about these ferrocenes is that all of the methylene tethers have expanded bond angles.[15] The C-C-C bond angles are closer to those of sp^2 (116°) rather than of sp^3 (109°). This expansion of the bond angle also occurs in a three pentamethylene tether ferrocene as well.[14] Thus far, no explanation has been offered as to why this occurs.

Another way that the ligands can be attached is in an intramolecular fashion in a metallic system. These could be as small as a binuclear system or expanded to include a polymer-like

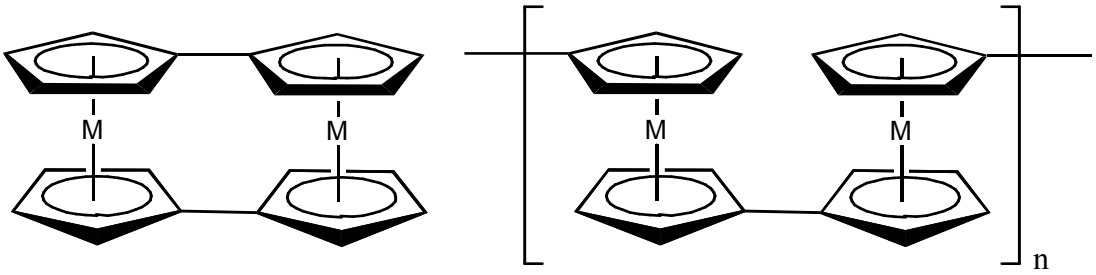

Figure 6: Polymer-like Metallocenophane Structures

system. A combination of these two structures (Figures 5 and 6) has also been reported by Hillman (Figure 7).[16]

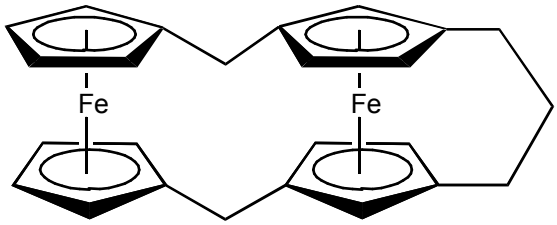

Figure 7: Multinuclear Metallocenophane Structure

Magnetism:[17]

Magnetism is a very broad subject, so for the purpose of this thesis, four types of magnetism will be discussed: paramagnetism, ferromagnetism, antiferromagnetism, and ferrimagnetism. A paramagnetic material has at least one unpaired electron in either an atomic or molecular orbital. When an external magnetic field is applied to a paramagnetic material, the unpaired electrons align with the field to produce a rather weak magnetic moment. Paramagnets do not retain magnetization once the magnetic field is removed because thermal jostling causes the molecular dipoles to be randomly oriented, which causes its magnetic properties to vary depending on the temperature.[18]

Ferromagnetism is the type of magnetism that is exhibited by permanent magnets. A ferromagnet has unpaired electrons that will align parallel with an external magnetic field like a paramagnet, but unlike the paramagnet, the spins also will align parallel with each other (Figure 8). Because the spins are aligned when the external field is removed, the magnetism is

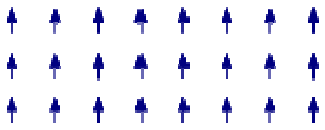

Figure 8: Ferromagnetic ordering of electron spins

retained. All of the spin alignment effects only occur at temperatures below the Curie temperature. Above the Curie temperature, a ferromagnetic substance loses its ferromagnetic properties; however, when it is cooled below the Curie temperature, the spins will once again align.[19]

In antiferromagnetism, the spins of the unpaired electrons are aligned but in opposing directions (Figure 9). Because of the opposing spins, substances exhibiting antiferromagnetism

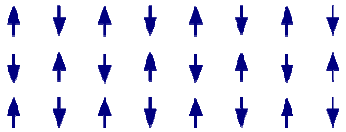

Figure 9: Antiferromagnetic ordering of electron spins

have no net magnetic moment. Substances that exhibit this type of magnetism only do so below the Néel temperature. Above the Néel temperature, these substances are usually paramagnetic.

Ferrimagnetism is similar to that of antiferromagnetism in that the unpaired electrons are aligned in opposing directions, although more electrons are aligned in one direction than the other, which are shown by the larger blue arrows in Figure 10. Because more of the electrons are aligned together, the substance will have a magnetic moment. Substances that exhibit

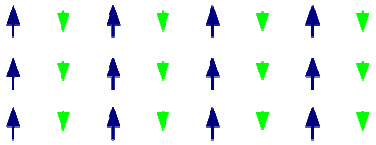

Figure 10: Ferrimagnetic ordering of electron spins

ferrimagnetism only do so below the Curie temperature. Because of the opposing spins, there is a temperature at which the magnetic moments will be equal. This temperature is called the magnetization compensation point.

Foundations for the Work Done on This Project:

In the late 1980s, Miller and Epstein found that the ionic compound $[(C_5Me_5)_2Fe][TCNE]$ (TCNE = tetracyanoethylene), once magnetized, retains externally induced magnetism for a short time.[20] This salt belongs to a class of substances, called ionic-charge transfer complexes,

that show magnetic behavior on the molecular scale. Miller and Epstein synthesized this compound to try to create a molecule with magnetism similar to that of iron.[20]

One question that arose after Miller and Epstein's discovery of $[(C_5Me_5)_2Fe][TCNE]$ ferromagnetism is what would happen to the magnetism if the symmetry was lowered but the electron density remained approximately constant.[20] Decamethylferrocene contains several degenerate orbitals because of its D_{5d} symmetry. If symmetry was reduced to a point group such as C_s, no degenerate orbitals would be present in the cation. Miller and Epstein did synthesize $[Fe(C_5Me_4H)_2]^+[A]^-$ (A = TCNE, TCNQ) (TCNQ = 7,7,8,8-tetracyano-*p*-quinodimethane).[21] Although this compound did lower the symmetry, it also greatly changed the electron density in the cation. Castellani and Yee synthesized $[Fe(C_5EtMe_4)_2]^+[TCNE]^-$, which keeps the electron density similar to the C_5Me_5 compound.[22] However, because the ethyl groups lie out of the plane of the cyclopentadienyl rings, the TCNE molecules are not parallel to the C_5 rings. This disruption in the crystal structure causes a major change in the magnetism. It is proposed to use [4]octamethylferrocene to form a charge-transfer salt with TCNE in an attempt to solve this problem.

Experimental Section

General Data. All air- and water-sensitive materials were handled under a nitrogen atmosphere using standard Schlenk techniques. Air-sensitive solids were handled under argon in a Vacuum Atmospheres glovebox equipped with a HE-493 dri-train. Diethyl ether was distilled from sodium/benzophenone ketyl under nitrogen. Hexane was purified by bubbling nitrogen through it to remove dissolved oxygen. Tetrahydrofuran was distilled from potassium/benzophenone ketyl under nitrogen. 2-Bromo-2-butene (Acros) was purified by passing it down a 1″ x 3″ 80-100 mesh basic alumina column. Dichloromethane was distilled from calcium hydride under nitrogen. *n*-Butyllithium (Aldrich), high sodium lithium wire (Aldrich), dimethyl adipate (Aldrich),

p-toluenesulfonic acid (Fischer), tetramethylcyclopentadiene (Norquay), and anhydrous iron(II) chloride (Strem) were used as received.

Preparation of $(C_5Me_4H)(CH_2)_4(C_5Me_4H)$.

Method 1

Preparation of $Li(C_5Me_4H)$. Diethyl ether (400 mL) was added to a Schlenk flask containing tetramethylcyclopentadiene (20.2 g, 165 mmol). The resulting solution was cooled in an acetone/liquid nitrogen bath to approximately -20 °C. *n*-Butyllithium (66 mL, 2.5 *M* in hexanes) was added over *ca.* 5 min with stirring and an off-white solid immediately began to form. The mixture was stirred overnight. The reaction mixture developed the consistency of a paste and more diethyl ether (100-200 mL) was added to make it fluid again. The solid was collected by filtration via a fritted funnel and dried *in vacuo,* yielding $Li(C_5Me_4H)$ as a white solid.[23] This material was used without further purification.

Preparation of $(C_5Me_4H)(CH_2)_4(C_5Me_4H)$. Diethyl ether (*ca*. 275 mL) was added to a Schlenk flask containing $Li(C_5Me_4H)$ (10.0 g, 77.6 mmol). The mixture was cooled in an ice bath and 1,4-dibromobutane (7.96 g, 37.0 mmol) was quickly added. A white solid rapidly formed, and the solution turned yellow. The mixture was stirred for three days. On the second day, an ^1H NMR spectrum showed a significant amount of remaining 1,4-dibromobutane. A ^1H NMR spectrum on the third day showed that 1,4-dibromobutane resonances were still present, but with much less intensity (*ca.* 10%). At this point, the solution was vacuum filtered to remove the solid, and the solvent was then removed from the filtrate *in vacuo* to yield a thick, opaque, yellow oil (8.15 g). This material was used without further purification. To estimate the purity of the salt, the solid by-product was treated with a silver nitrate solution, and the resulting silver bromide was weighed. It suggested a purity of *ca*. 50%

Method 2

Preparation of $(C_5Me_4H)(CH_2)_4(C_5Me_4H)$.[24] Diethyl ether (*ca*. 25 mL) was added to a 3-neck flask (equipped with a pressure-equalized dropping funnel and water condenser) containing

lithium (5.6 g, 810 mmol) that had been cut into 1/8 inch pieces. 2-Bromo-2-butene (50.2 g, 372 mmol) was placed into the addition funnel. A small amount (*ca.* 1-2 mL) of 2-bromo-2-butene was added to the flask to initiate the reaction. Once the reaction started, diethyl ether (225 mL) was added through the reflux condenser. The 2-bromo-2-butene was added dropwise to maintain a gentle reflux. The mixture was stirred for 2 hr and turned orange. Dimethyl adipate (DBE-6 dibasic ester, 17 g, 97 mmol) was placed into the addition funnel and added dropwise to the reaction mixture while maintaining a gentle reflux. The reaction mixture turned yellowish-orange during the addition, but after it was stirred for 2 hr, it had turned back to orange. A saturated ammonium chloride solution (150 mL) was placed into the dropping funnel and slowly added to maintain a gentle reflux. The mixture was stirred for 1.5 hr, then poured into a separatory funnel containing a saturated ammonium chloride solution (*ca*. 250 mL). The aqueous layer was removed and adjusted to pH 9 with concentrated hydrochloric acid and then extracted twice with diethyl ether. The ether layers were combined and dried overnight over anhydrous magnesium sulfate. The mixture was filtered, and the volume was reduced *in vacuo* to 50 -100 mL. Diethyl ether (70 mL) was added to a 3-neck flask (equipped with a pressure-equalized dropping funnel and water condenser) containing *p*-toluenesulfonic acid (3.8 g, 20 mmol) that had been ground in a mortar and pestle. The solution that was reduced was then placed into the dropping funnel and quickly added to the acid to maintain a reflux. Two layers formed: the ether layer was orange and the aqueous layer was black. The mixture was stirred for 2 h. The mixture was washed twice with a saturated sodium bicarbonate solution. The aqueous layers were combined and extracted twice with diethyl ether. The ether layers were combined and dried over anhydrous magnesium sulfate. The mixture was filtered, and the solvent was removed *in vacuo* leaving an orange oil (22.9 g).

Preparation of $Li_2[(C_5Me_4)(CH_2)_4(C_5Me_4)]$. Tetrahydrofuran (*ca*. 600 mL) was placed into a Schlenk flask with the 1,4-bis(2,3,4,5-tetramethylcyclopentadienyl)butane (22.9 g, 76.9 mmol) obtained in the previous preparation and cooled to -20 °C in an acetone/liquid nitrogen

bath. *n*-Butyllithium (100 mL, 1.6 *M* in hexane, 160 mmol) was added . An orange solid formed quickly and the mixture was stirred for 1.5 hr. The solid was filtered via a fritted funnel and dried *in vacuo* leaving lithium [*m*-[(1,4-butanediyl)tetramethyldi-2,4-cyclopentadien-1-ylidene]] as a white solid (20.3 g).

Preparation of [(C_5Me_4)(CH_2)$_4$(C_5Me_4)]Fe. Lithium [*m*-[(1,4-butanediyl)tetramethyldi-2,4-cyclopentadien-1-ylidene]] (3.06 g, 10.1 mmol) was placed into a Schlenk flask with anhydrous ferrous chloride (1.28 g, 10.1 mmol) and cooled to approximately -80 °C in an acetone/liquid nitrogen bath. Tetrahydrofuran (50 mL) was added quickly, yielding a light brown mixture that was stirred overnight and while being allowed to warm to room temperature. The solvent was removed *in vacuo* leaving a sticky black solid. Hexane (*ca*. 25 mL) was added to extract the product, and the resulting mixture was stirred for *ca.* 30 min. The mixture was filtered via cannula, and the solvent was removed *in vacuo* leaving a yellow oil. Hexane (10 mL) was added to the flask and then cooled in an acetone/dry ice bath for 9 h yielding a yellow-orange solid. The mixture was filtered via cannula and the solid was dried *in vacuo* overnight. The solid was sublimed with a 100 ºC bath twice, once for 15 h and again for 3 h. The materials on the cold-finger were dried separately *in vacuo* overnight. Each sublimation yielded 0.04 g of product (0.1 mmol) that were separately recrystallized in pentane (1 mL each) at -40 °C. The orange crystals (0.07 g, 2% yield) recovered were then combined: Mp: 254-255 °C (dec.), UV-vis max (CH_2Cl_2) 420 nm, 300 (sh), NMR (CD_2Cl_2) ^{1}H: δ 1.59 (s, CH_3), 1.67 (s, CH_3), 1.72 (br s, CH_2), 2.18 (br s, CH_2); ^{13}C: δ 9.5 (CH_3), 9.6 (CH_3), 27.57 (CH_2), 27.65 (CH_2), 78.8 (Cp), 83.9 (Cp). Anal. Calcd for $C_{22}H_{32}Fe$: C, 75.00; H, 9.15; Fe, 15.85. Found: C, 74.83; H, 9.28. Crystals suitable for X-ray diffraction were grown in pentane at -40 °C.

Preparation of [[(C_5Me_4)(CH_2)$_4$(C_5Me_4)]Fe][TCNE]. Dichloromethane (1.5 mL) was placed into a crystallization tube with [4]octamethylferrocenophane (0.213 g, 0.605 mmol). In a separate crystallization tube, tetracyanoethylene (0.086 g, 0.671 mmol) was dissolved in dichloromethane (6 mL). The TCNE solution was added via cannula to the ferrocene solution

and stirred for 30 min, forming an olive green solution. The solution was reduced in volume to *ca*. 4 mL *in vacuo*, then layered with hexane (4 mL), and left to crystallize for 1 week. The mixture was filtered via cannula and dried *in vacuo* to yield a black solid . The mother liquor was evaporated to half its original volume. The solution was layered with hexane (5 mL) and left to crystallize for one week. The mixture was filtered via cannula, and the solid was dried *in vacuo*. The black solids (0.103 g, 35% yield) recovered were then combined. The microcrystalline product was not suitable for crystallographic analysis.

Preparation of $[[(C_5Me_4)(CH_2)_4(C_5Me_4)]Co][PF_6]$.[25] Lithium[*m*-[(1,4-butanediyl)tetramethyldi-2,4-cyclopentadien-1-ylidene]] (1.01 g, 3.25 mmol) was placed into a Schlenk flask with anhydrous cobalt(II) chloride (0.432 g, 3.33 mmol). Tetrahydrofuran (25 mL) was added quickly yielding a dark blue solution that was stirred overnight. Ammonium hexafluorophosphate (0.575 g, 3.53 mmol) was placed into a separate Schlenk flask. The cobalt solution was transferred via cannula onto the ammonium hexafluorophosphate. Gas was produced, yielding a purple solution that was stirred overnight. The solvent was removed *in vacuo* leaving a purple solid. The solid was extracted with dichloromethane (*ca.* 25 mL) and vacuum filtered. The volume was reduced *ca*. 5-10 mL and layered with hexane. The mixture was left to crystallize for one week. The solid was vacuum filtered and dried *in vacuo* to yield a purple solid.

Computational Method

All calculations were done using the B971 density functional method with a 6-31G basis set with polarization on the *d* orbitals The initial coordinates for both the [4]ferrocenophane and the [4]octamethylferrocenophane minimal structures were optimized by a member of Dr. Burcl's group, Ms. Candice Dotson, using the method and basis set described above.

Results and Discussion

Initially, a modified Bercaw *et al*.[24] synthesis was used, but because of frequent failure of this synthetic method and low yields on the few attempts that did yield product, another pathway

to 1,4-bis(2,3,4,5-tetramethylcyclopentadienyl)butane was developed based on the method of Lüttringhaus and co-workers.[12,22] It proceeded by the following two reactions (eq. 3 and 4) in an maximum 75% overall yield. The actual yield is lower because no purification was attempted in either reaction.

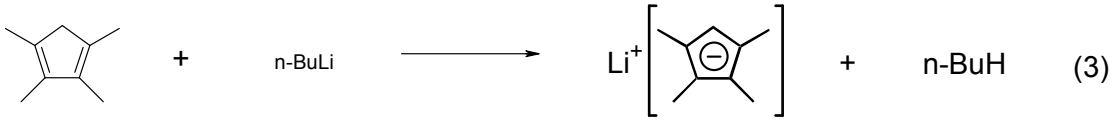

(3)

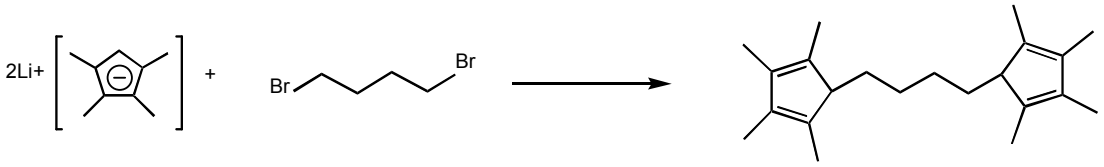

(4)

The ^{1}H and ^{13}C NMR spectra confirmed the preparation of the 1,4-bis(2,3,4,5-tetramethylcyclopentadienyl)butane (see Figures 21-23 in the Appendix). The ^{1}H and ^{13}C NMR spectra of 1,4-bis(2,3,4,5-tetramethylcyclopentadienyl)butane showed significant amounts of impurities. Some of these impurities were probably isomeric products that arose from reactions in eq 3 and 4. The impurities that were just upfield of 1 ppm probably resulted from the hydrocarbon grease that was used on the reaction flask. To further investigate the problem with the impurities, some of the lithium [*m*-[(1,4-butanediyl)tetramethyldi-2,4-cyclopentadien-1-ylidene]] was washed with a 1% solution of silver nitrate, a white solid was formed. When the solid was weighed, it was determined that approximately half of the lithium salt was lithium bromide. The lithium bromide formed because the lithium tetramethylcyclopentadienide only added to one side of the 1,4-dibromobutane instead of both sides. This meant that when the *n*-butyllithium was added, that a butyl group was added and lithium bromide formed. From this data, it was concluded that the impurities that occurred in the spectra of 1,4-bis(2,3,4,5-tetramethylcyclopentadienyl)butane accounted for roughly half of the yield, thereby lowering the yield to *ca*. 35%.

When the poor yield and difficult separation of the above method were realized, another route to synthesize 1,4-bis(2,3,4,5-tetramethylcyclopentadienyl)butane was attempted which involved modifying a sequence of reactions similar to that employed by Bercaw, *et al*. (eq 5-7).[21]

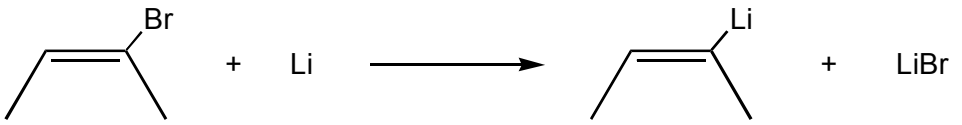

(5)

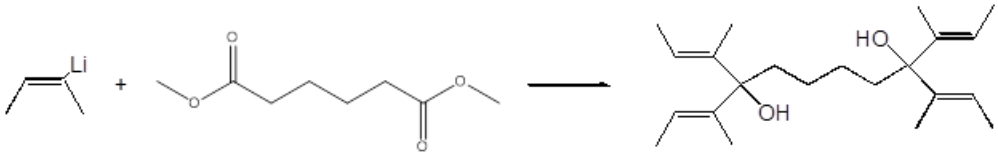

(6)

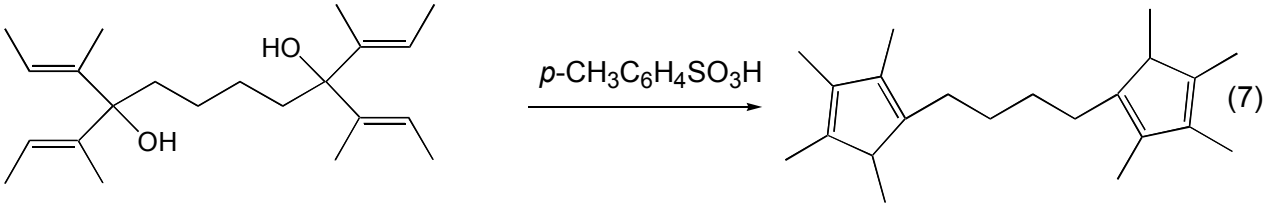

(7)

Tobita and coworkers[26] successfully employed this method in the synthesis of 1,3-bis(2,3,4,5-tetramethylcyclopentadienyl)propane. After several attempts, this yielded the desired product.

[4]Ferrocenophane was then synthesized by the following reaction, which was similar to a synthesis employed by Lüttringhaus, *et al*.:[12]

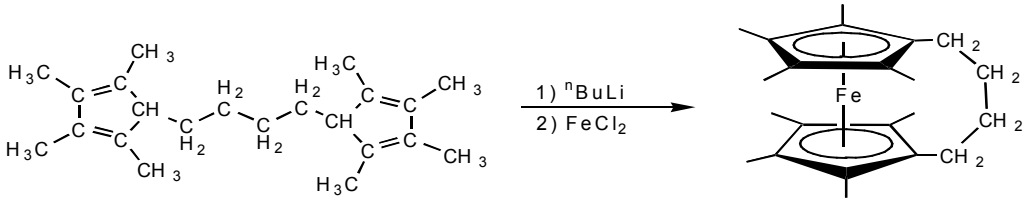

(8)

This reaction produced an orange crystalline solid in about 2% yield. This was a low yield even when compared to other methods of synthesizing tethered ferrocenes, where yields varied anywhere from 12 to 34%.[27] This low yield may arise, in part, from side reactions because the ferrocene product was initially mixed in an orange oil. Attempts to sublime and to crystallize the ferrocene out of the oil were unsuccessful. A stream of air was drawn over damp crystals

overnight caused oxidation of the ferrocene, suggesting that it is slightly air-sensitive. The ferrocenophanes tend to be more air-sensitive depending on the dihedral angle of the cyclopentadienyl rings, with the larger the angle, the more air-sensitive the compound.[11] When the dihedral angle of the rings is close to zero, as in ferrocene, is when the bonds are the strongest. As this angle increases, the bond energy decreases and destabilizes the product thereby increasing the air-sensitivity. ^{1}H and ^{13}C NMR spectra (Figures 24 and 25), as well as X-ray crystallography (Figure 26 and Table I) are reported here. The dihedral angle between the cyclopentadienyl rings is 1°. The C-C-C angles in the tether are all expanded and approach that of an sp^2 carbon. An electronic spectrum, elemental analysis, and the decomposition temperature were obtained for the ferrocene and reported in the Experimental Section (*vide supra*). In the ^{1}H spectrum of [4]ferrocenophane, the resonances that correspond to the methylene groups are broad. Hillman and coworkers[14] suggested this occurs because in the non-methylated, four-methylene tether ferrocene, the tether twists rapidly. According to Hillman, when the bridges flip rapidly, two groups of peaks occur in the spectrum. Hillman *et al*. also reported that the disorder in the backbone had not fully been investigated. For more information about this, see the computational section (*vide infra)*.

Suitable crystals for cystallgraphy have not been grown for either 1,1'-(tetramethylene)octamethylferrocenium tetracyanoethanide or the 1,1'-(tetramethylene)octamethylcobaltocenium hexafluorophosphate. The synthesis that has been reported (*vide supra*) is still in progress.

Computational Results

One question that came from this research was whether or not the carbon tether would flip rapidly on the NMR time scale. To answer this question, the energy for the transition and intermediate states had to be calculated. For the [4]ferrocenophane, there are three transition states, two intermediates and two structures of minimum energy; however, two of the transition states have the same energy because they are equivalent relative to a plane of symmetry. The

minimum energy structures were taken to be zero energy and all of the transition state energies are reported relative to that. The ΔG's are given in kcal/mol at 25 °C. For a full listing of thermodynamic data, refer to the corresponding table in the Appendix.

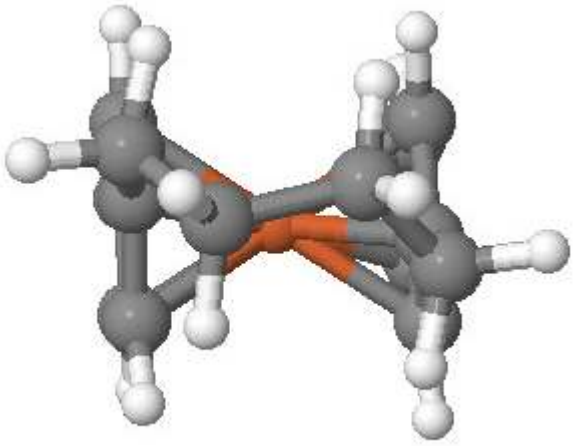

Figure 11: Minimum energy structure for [4]Ferrocenophane

ΔG=6.21 kcal/mol for the first activation barrier.

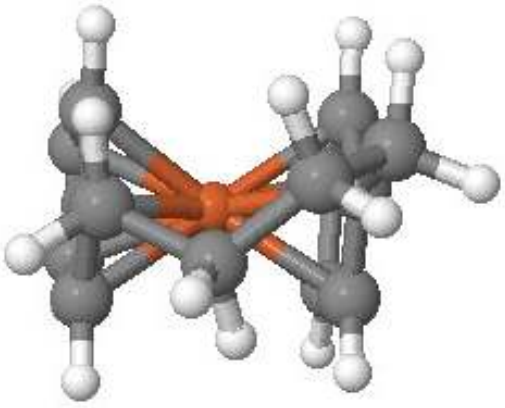

Figure 12: 1st Transition state for [4]Ferrocenophane

ΔG=4.85 kcal/mol to get down to the intermediate.

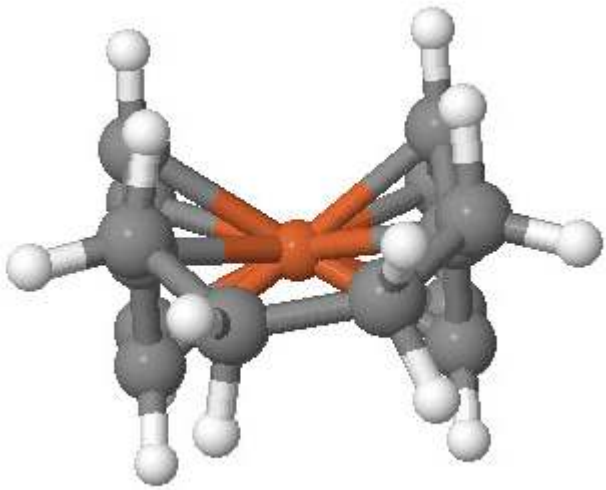

Figure 13: Intermediate state for [4]Ferrocenophane

ΔG=2.56 kcal/mol to go from the intermediate to the middle transition state

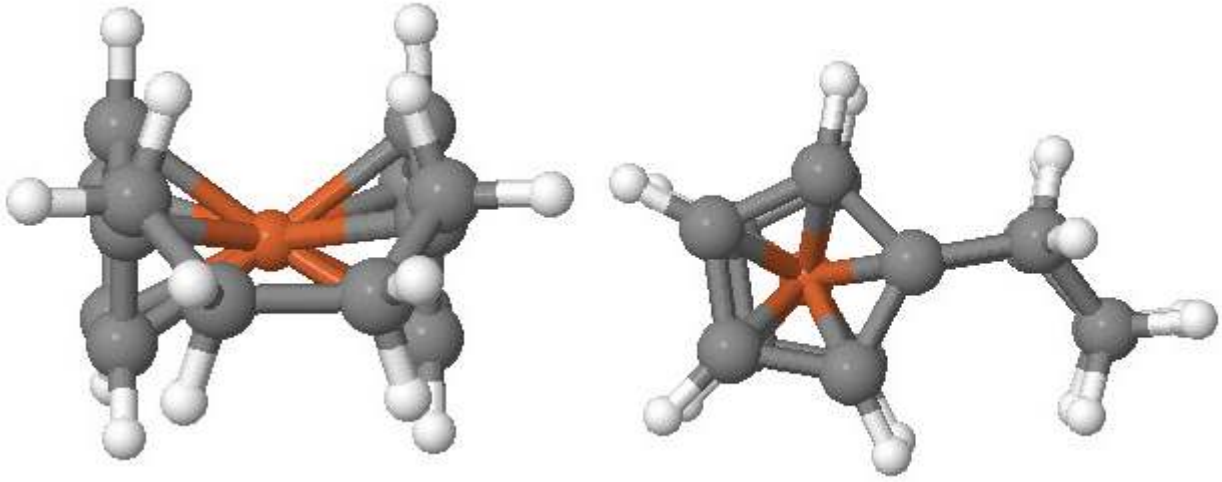

Figure 14: middle transition state for [4]Ferrocenophane

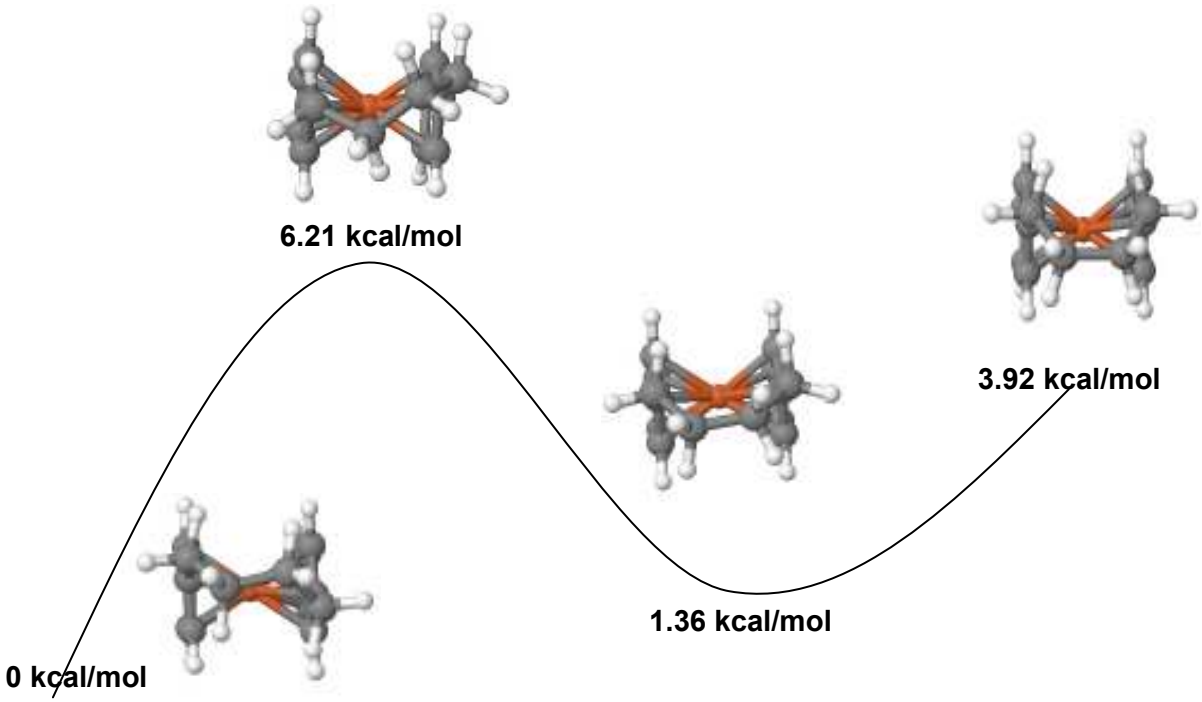

Figure 15: The Potential Energy Curve for [4]Ferrocenophane

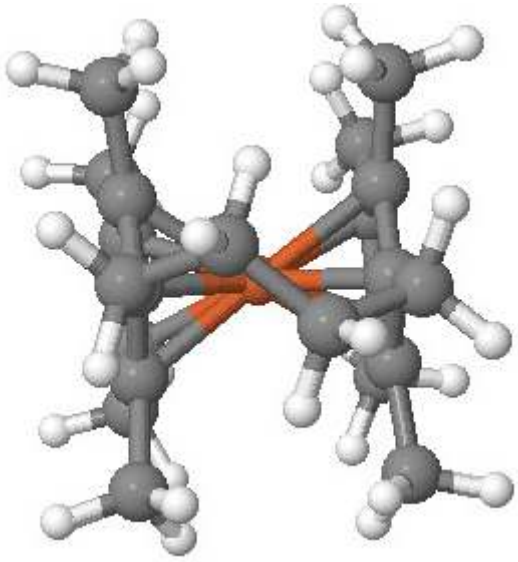

Figure 16: Methylated minimum energy structue for [4]OctamethylFerrocenophane

ΔG=6.64 kcal/mol for the first activation barrier.

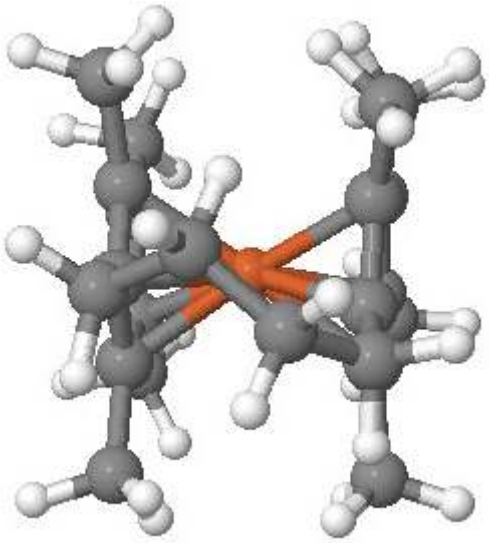

Figure 17: methylated 1st transition state for [4]OctamethylFerrocenophane

ΔG=2.33 kcal/mol to go from the transition state to the intermediate

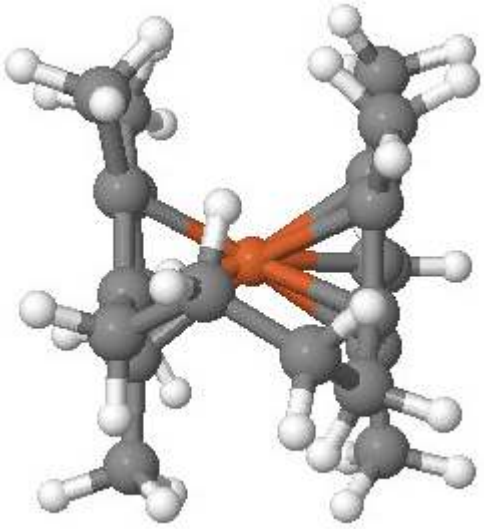

Figure 18: methylated intermediate for [4]OctamethylFerrocenophane

ΔG=3.60 kcal/mol to go from the intermediate to the middle transition state

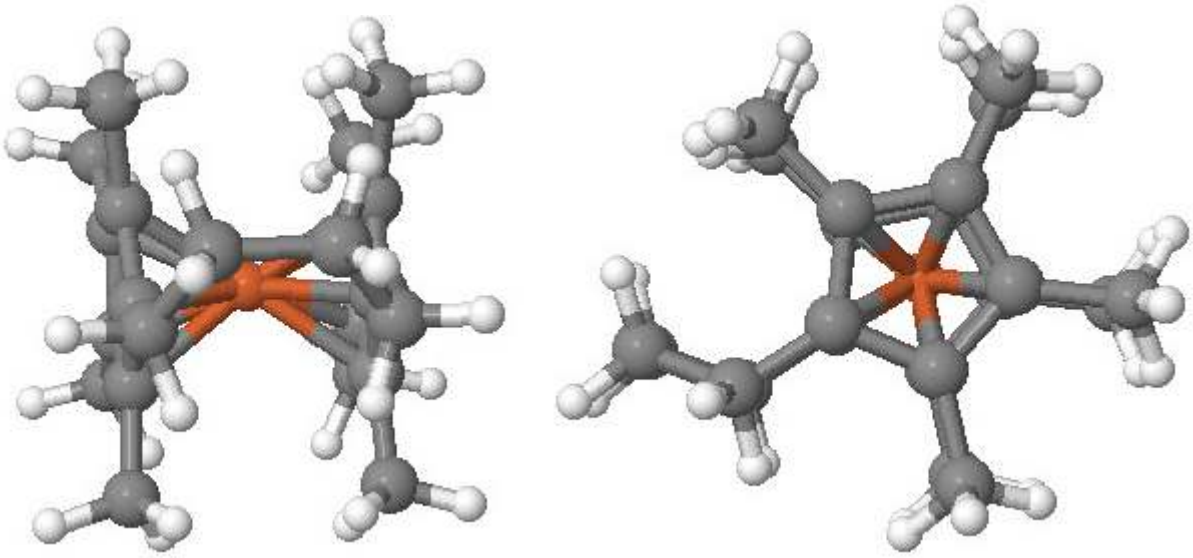

Figure 19: methylated middle transition state for [4]OctamethylFerrocenophane

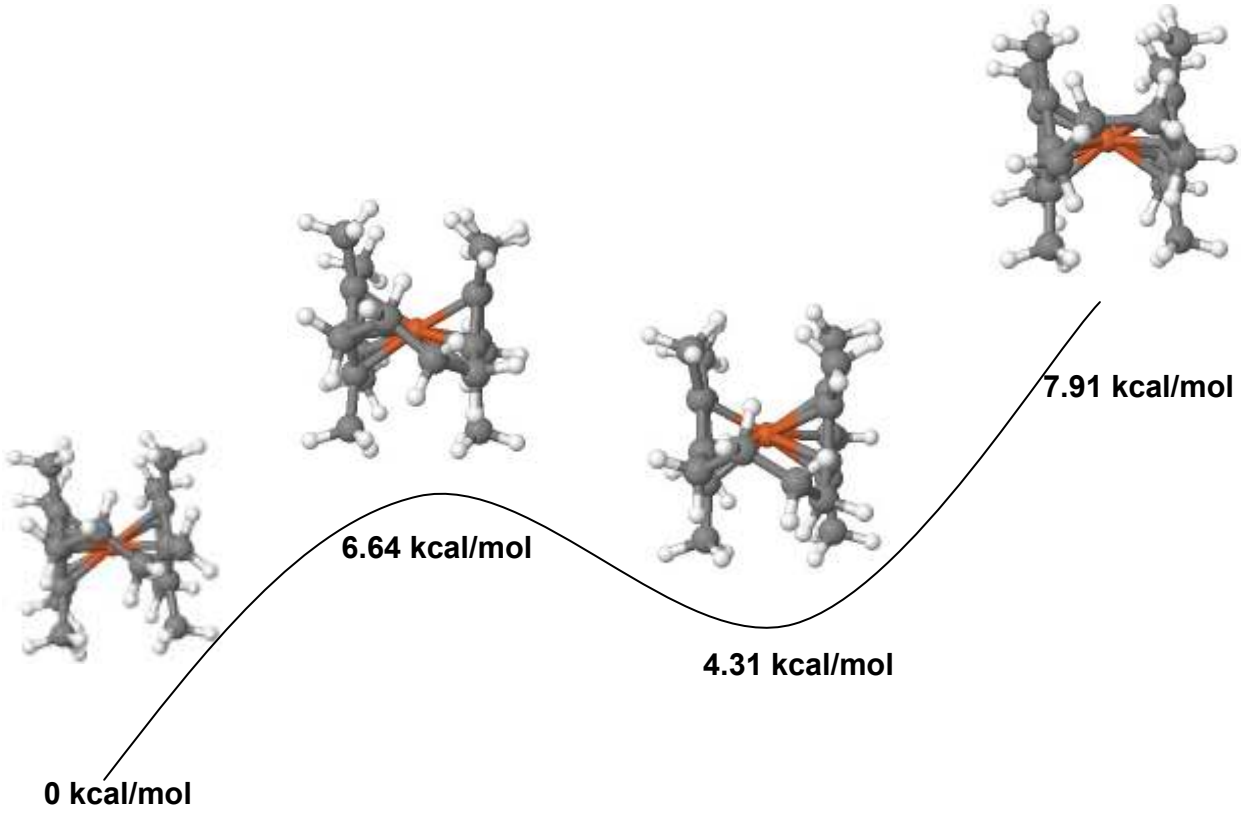

Figure 20: Potential Energy Curve [4]Octamethylferrocenophane

For the [4] ferrocenophane, the energy of the middle transition state (Figure 14) is considerably lower than that of the first transition state (Figure 12) and because of this it is unlikely that either of the intermediates would be observed. The only way that these intermediates would, in principle, be observed is if the molecule lost or transferred some energy by colliding with another molecule once it had reached the transition state. The potential energy curve of [4]octamethylferrocenophane (Figure 20) has some differences when compared to that of [4]ferrocenophane (Figure 15). By adding methyl groups to the cyclopentadienyl ring, the middle transition state increases in energy to be larger than that of the first transition state. This occurs because the electron densities of the methyl groups start to overlap the electron density of the methylene groups of the tether.

The low activation energy for the transition between minimum structures, 6.21 kcal/mole for [4]Ferrocenephane and 7.91 kcal/mole for [4]Octamethylferrocenephane, suggests that the energy barrier is low enough for the tethers on both of the compounds reported here to flip rapidly on the NMR time scale and should be observed as a broad singlet in the NMR.

Conclusions

In conclusion, 1,4-bis-(2,3,4,5-tetramethylcyclopentadienyl)butane has been synthesized by two methods. This molecule was deprotonated and reacted with ferrous chloride to make [4]octamethylferrocenophane, which was characterized using NMR, electronic spectroscopy, elemental analysis, and X-ray crystallography. The cyclopentadienyl rings are 1° from parallel planar, which suggests that this compound should have the proper stacking to form the desired charge-transfer salt, 1,1'-(tetrametylene)octamethylferrocenium tetracyanoethanide. An attempt to synthesize this charge-transfer salt yielded no suitable crystals for crystallographic analysis. A computational study was done on both [4]ferrocenophane and [4]octamethylferrocenophane to determine what the potential energy surface is for both molecules going between their minimum energy structures. From these surfaces, it was determined that the carbon tether in both structures would flip rapidly on the NMR time scale.

Appendix

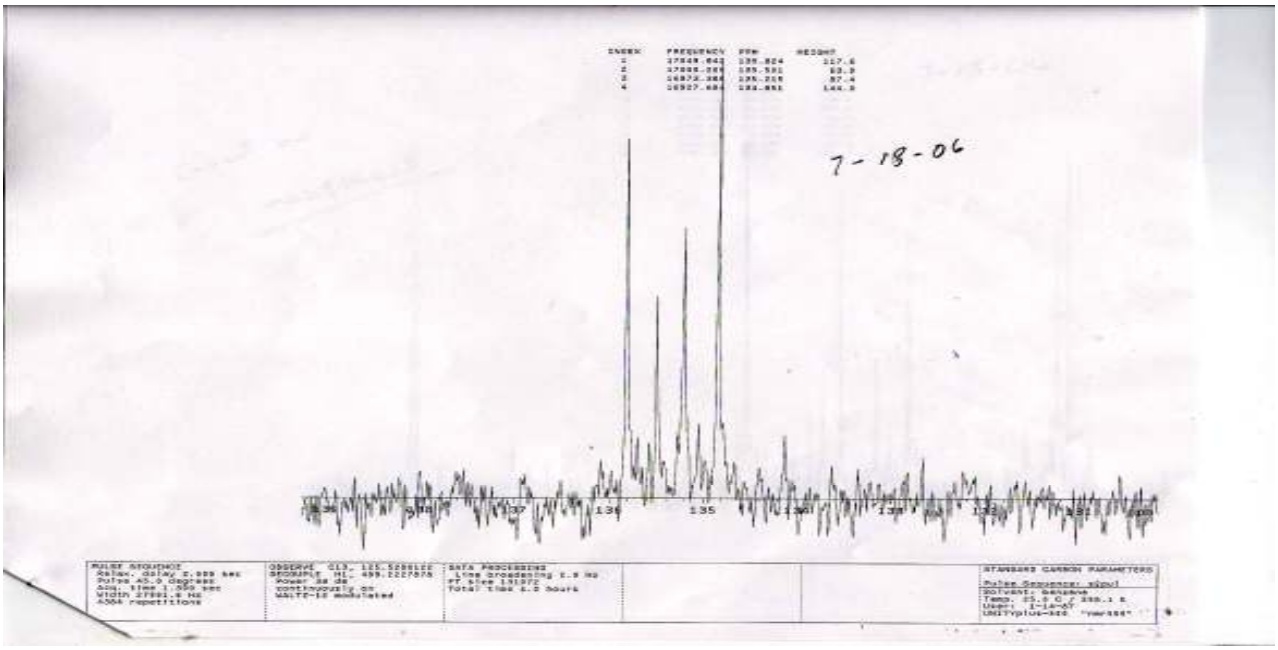

Figure 21: ^{13}C spectrum of 1,4-bis(2,3,4,5-tetramethylcyclopentadienyl)butane in d_6-benzene from 130-140 ppm

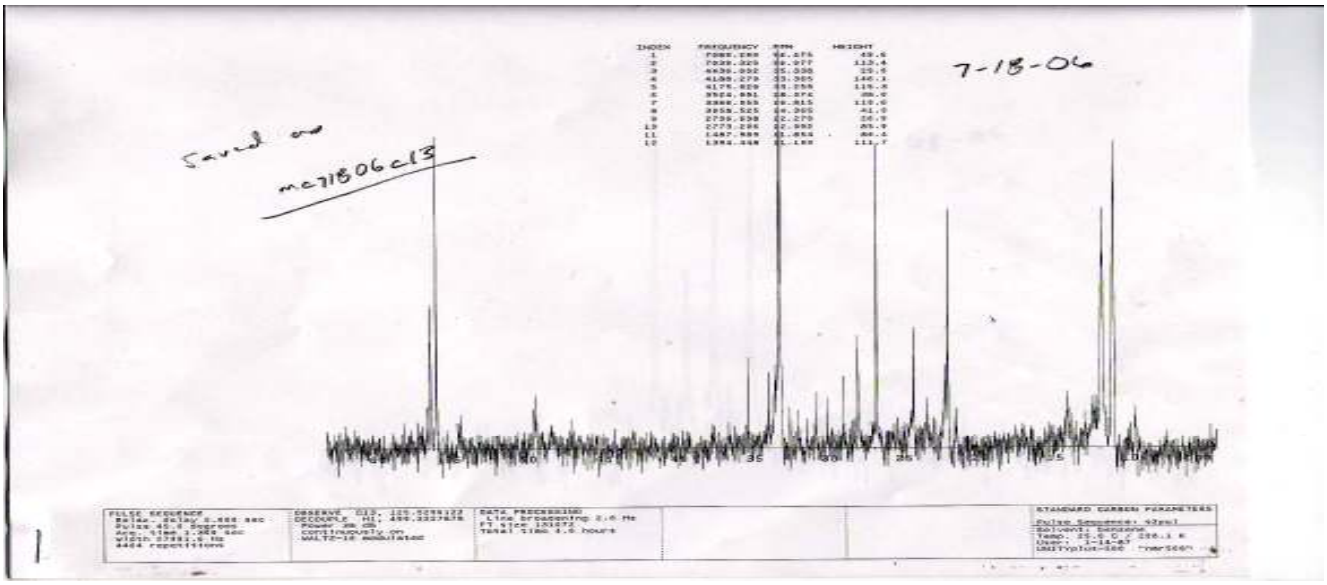

Figure 22: ^{13}C spectrum of 1,4-bis(2,3,4,5-tetramethylcyclopentadienyl)butane in d_6-benzene from 0-60 ppm

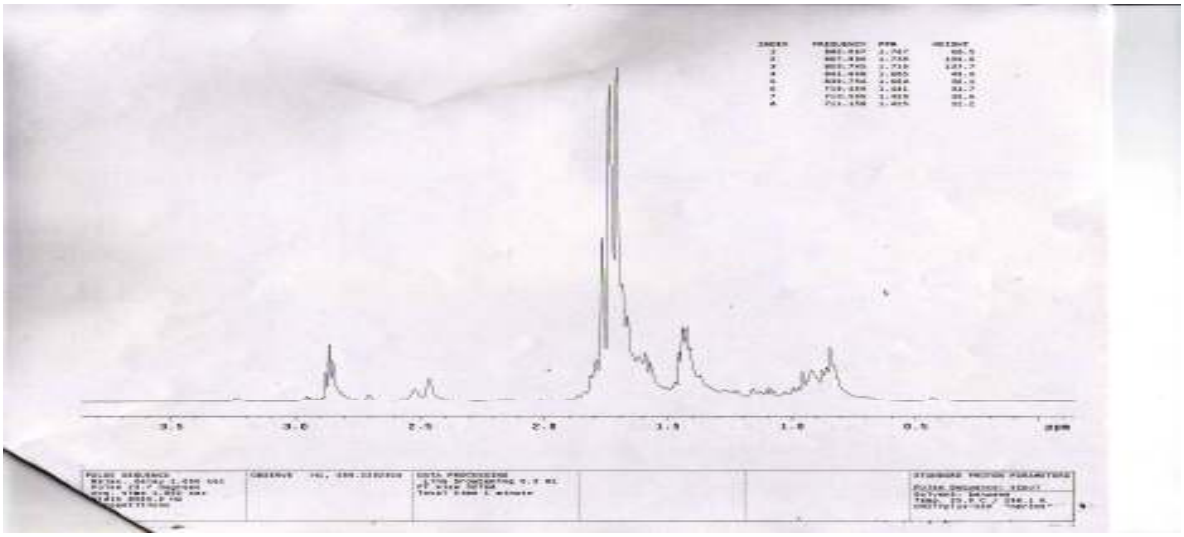

Figure 23: ^{1}H spectrum of 1,4-bis(2,3,4,5-tetramethylcyclopentadienyl)butane in d_6-benzene from 0-4 ppm

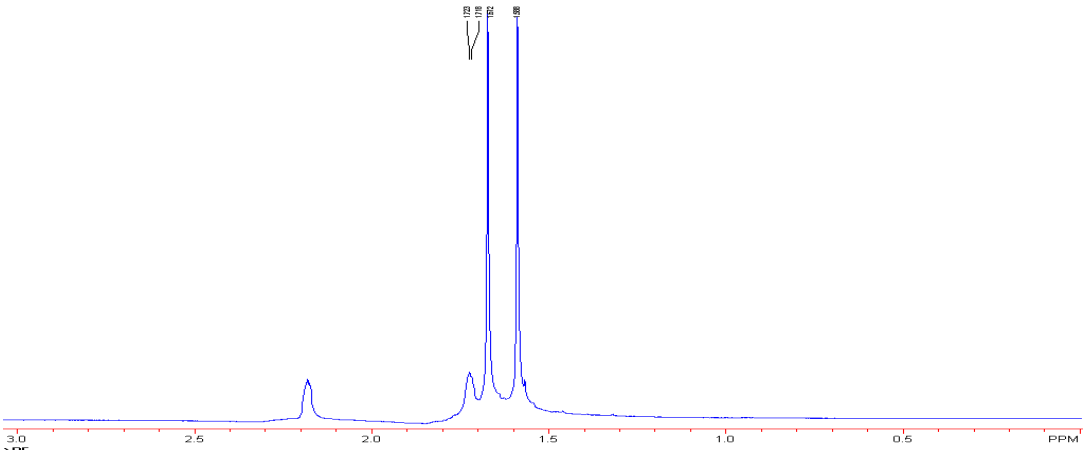

Figure 24: H^{1} spectrum of [4] ferrocenophane in CD_2Cl_2 from 0-3 ppm

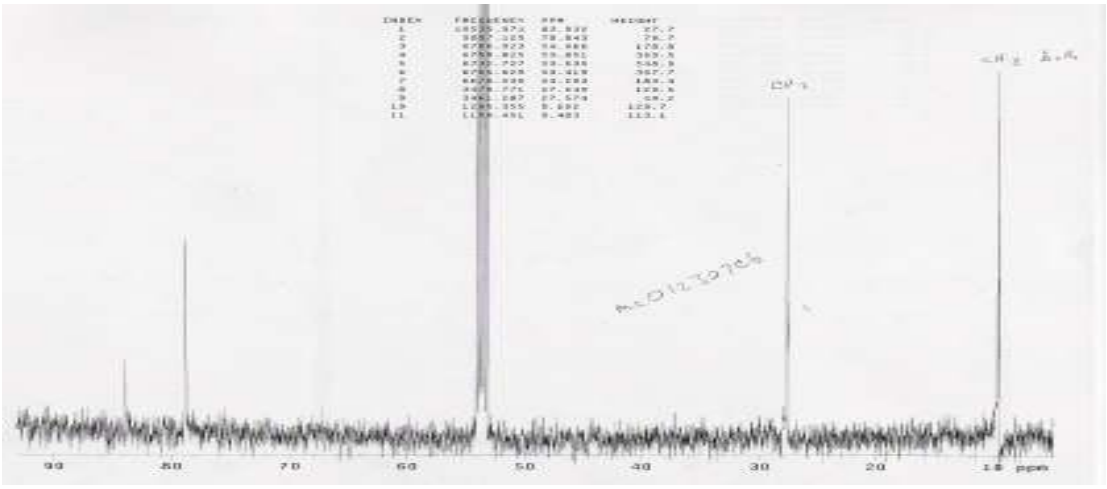

Figure 25: C^{13} spectrum of [4] ferrocenophane in CD_2Cl_2 from 0-90 ppm

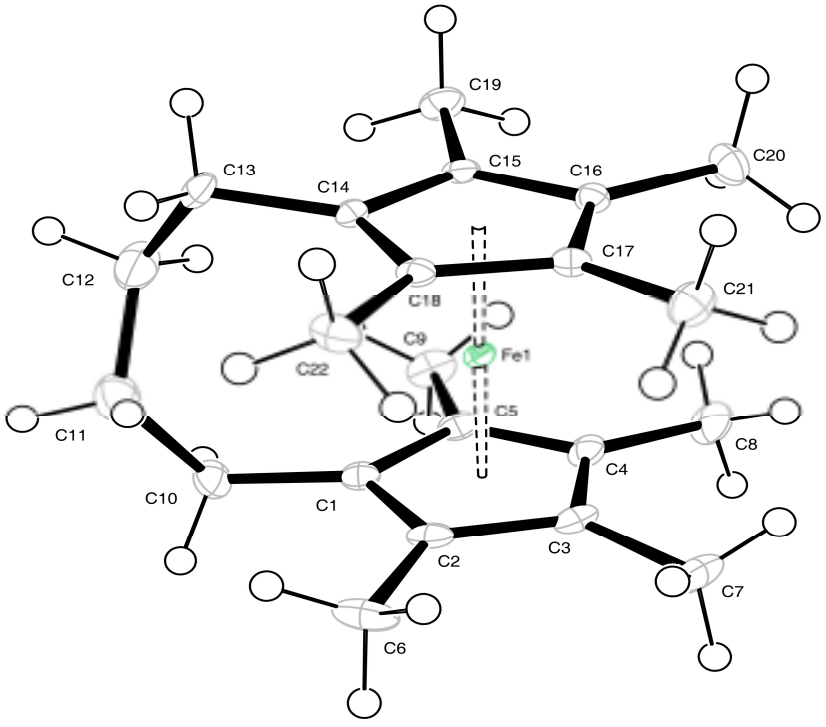

Figure 26: Crystal Structure of [4]Ferrocenophane

Bond Angles	
C1-C10-C11	117.4
C10-C11-C12	116.4
C11-C12-C13	114.2
C12-C13-C14	116.6
Cp rings (dihedral)	1.0

Table I: Bond Angles for [4]Octamethylferrocenophane

	[4]ferrocenophane					
Zeropoint kJ/mol	660.57					
	S J/mol*K	Cp J/mol*K	ddH kJ/mol	SCF	dG kJ/mol	dG kcal/mol
100	296.29	75.6	4.92	-4738415.04	24.92	5.96
200	370.64	150.75	16.07		25.29	6.05
298.15	446.8	237.12	35.08		25.96	6.21
300	448.28	238.75	35.52		25.98	6.21
400	528.58	321.41	63.63		26.92	6.44
500	607.89	389.36	99.3		28.06	6.71
600	683.83	443.23	141.03		29.35	7.02
700	755.5	486.31	187.59		30.77	7.36
800	822.81	521.49	238.03		32.33	7.73
900	885.98	550.73	291.69		33.99	8.13
1000	945.31	575.33	348.02		35.73	8.55

Table II: ΔG for Minimum Structure

	transition1 for [4]ferrocenophane					
Zeropoint kJ/mol	659.6					
	S	Cp	ddH	SCF	dG	dG kcal/mol
100	294.61	71.37	4.76	-4738389	18.78	4.49
200	365.23	144.2	15.36		19.33	4.62
298.15	438.58	229.7	33.67		20.27	4.85
300	440.01	231.32	34.1		20.29	4.85
400	518.12	313.64	61.45		21.54	5.15
500	595.67	381.42	96.33		23.00	5.50
600	670.15	435.15	137.26		24.63	5.89
700	740.58	478.14	183		26.41	6.32
800	806.79	513.25	232.63		28.33	6.78
900	868.98	542.43	285.46		30.34	7.26
1000	927.44	566.99	340.96		32.44	7.76

Table III: ΔG for 1st Transition State

	Intermediate for [4]ferrocenophane					
Zeropoint kJ/mol	659.66					
	S	Cp	ddH	SCF	dG	dG kcal/mol
100	297.34	77.97	5.02	-4738408	7.62	1.82
200	373.05	152.15	16.36		8.94	2.14
298.15	449.68	238.15	35.48		10.69	2.56
300	451.16	239.78	35.92		10.72	2.57
400	531.74	322.29	64.13		12.81	3.06
500	611.23	390.12	99.88		15.12	3.62
600	687.29	443.84	141.68		17.59	4.21
700	759.06	486.81	188.29		20.22	4.84
800	826.43	521.88	238.78		22.97	5.50
900	889.63	551.03	292.47		25.82	6.18
1000	948.99	575.56	348.84		28.76	6.88

Table IV: ΔG for Intermediate

	Midtransition for [4]ferrocenophane			
Zeropoint kJ/mol	660.02			
	S	Cp	ddH	SCF
100	287.47	69.52	4.48	-4738401
200	357.13	143.3	14.95	
298.15	430.23	229.33	33.2	
300	431.65	230.96	33.62	
400	509.7	313.52	60.95	
500	587.24	381.41	95.83	
600	661.72	435.19	136.76	
700	732.16	478.2	182.51	
800	798.38	513.3	232.14	
900	860.57	542.49	284.97	
1000	919.04	567.04	340.48	

Table V: ΔG for the Middle Transition State

	[4]octamethylferrocenophane					
Zeropoint kJ/mol	1215.23					
	S J/mol*K	Cp J/mol*K	ddH kJ/mol	SCF	dG	dG kcal/mol
100	375.43	179.98	9.17	-5563211.71	25.45	6.09
200	545.91	321.51	34.57		26.44	6.32
298.15	697.45	445.76	72.23		27.77	6.64
300	700.21	448.1	73.05		27.81	6.65
400	846.15	570.67	124.07		29.44	7.04
500	985.42	678.75	186.69		31.27	7.48
600	1117.45	769.54	259.24		33.29	7.96
700	1241.94	845.38	340.1		35.43	8.48
800	1359.11	909.22	427.92		37.71	9.02
900	1469.42	963.36	521.62		40.09	9.59
1000	1573.37	1009.52	620.33		42.56	10.18

Table VI: ΔG for the Minimum Structure

	transition1 for [4]octamethylferrocenophane					
Zeropoint kJ/mol	1214.64					
	S	Cp	ddH	SCF	dG	dG kcal/mol
100	368.08	174.2	8.8	-5563186	7.25	1.74
200	533.93	314.05	33.52		8.30	1.98
298.15	682.37	437.79	70.41		9.72	2.33
300	685.09	440.12	71.23		9.76	2.33
400	828.69	562.42	121.44		11.51	2.75
500	966.11	670.36	183.22		13.46	3.22
600	1096.6	761.11	254.93		15.59	3.73
700	1219.79	836.95	334.94		17.85	4.27
800	1335.84	900.8	421.92		20.25	4.85
900	1445.15	954.95	514.78		22.76	5.45
1000	1548.22	1001.13	612.65		25.35	6.06

Table VII: ΔG for the 1st Transition State

	Intermediate for [4]octamethylferrocenophane					
Zeropoint kJ/mol	1214.92					
	S	Cp	ddH	SCF	dG	dG kcal/mol
100	375.73	181.21	9.23	-5563193	13.80	3.30
200	546.82	322.05	34.72		14.16	3.39
298.15	698.52	446.08	72.42		15.05	3.60
300	701.29	448.41	73.25		15.07	3.60
400	847.29	570.85	124.29		16.31	3.90
500	986.6	678.85	186.92		17.79	4.26
600	1118.64	769.61	259.48		19.44	4.65
700	1243.14	845.43	340.35		21.24	5.08
800	1360.32	909.26	428.17		23.18	5.55
900	1470.63	963.39	521.87		25.24	6.04
1000	1574.58	1009.55	620.58		27.36	6.55

Table VIII: ΔG for the Intermediate Structure

	Midtransition for [4]octamethylferrocenophane			
Zeropoint kJ/mol	1216.06			
	S	Cp	ddH	SCF
100	376.34	170.54	8.89	-5563180
200	539.87	311.59	33.29	
298.15	687.58	436.47	70.01	
300	690.29	438.82	70.82	
400	833.59	561.66	120.92	
500	970.87	669.87	182.65	
600	1101.29	760.73	254.31	
700	1224.43	836.62	334.29	
800	1340.43	900.49	421.24	
900	1449.7	954.65	514.07	
1000	1552.74	1000.83	611.9	

Table IX: ΔG for the Middle Transition State

Minima 1 with no methyls			
Fe	-0.25076451	0.756285871	-0.06374137
C	1.78858606	0.727041062	-0.08162706
C	1.31349087	2.077764774	-0.09786255
C	0.5186718	2.279767773	1.073824254
C	0.50498799	1.052706343	1.808367386
C	1.2801829	0.076476383	1.093858287
H	2.40348347	0.267767445	-0.84641367
H	1.50731351	2.810466227	-0.87175962
H	0.00360794	3.192656382	1.346714657
H	-0.02532445	0.8717445	2.736396597
H	0.83605384	-1.59705995	2.340144572
C	-1.87258301	-0.4744499	0.060049683
C	-1.0190636	-0.86450292	-1.02751051
C	-0.93967734	0.259487714	-1.91904519
C	-1.71573572	1.332357394	-1.3785598
C	-2.2932451	0.877828961	-0.15163137
H	-2.13220143	-1.08692356	0.915272338
H	-1.15551103	-2.8709468	-1.7041355
H	-0.35947994	0.291048693	-2.83424417
H	-1.82999594	2.318621418	-1.81139164
H	-2.92268496	1.458834889	0.51136059
C	-0.3888719	-2.21561563	-1.26188643
H	0.39375428	-2.11197073	-2.02699949
H	2.08835956	-3.30414355	0.938637314
C	0.20711294	-2.94024052	-0.03445784
H	-0.52123963	-2.94415255	0.789696285
H	0.33017736	-3.99317862	-0.32276718
C	1.57693155	-2.44220428	0.488692529
H	2.20567949	-2.13771725	-0.36084346
H	2.54708813	-1.32623704	2.058017036
C	1.56434539	-1.33012419	1.561053761

Table X: Coordinates of the 1st Minimum Structure

Minima 2 with no methyls			
Fe	-0.250626071	0.756218408	0.063831674
C	0.504787536	1.052700567	-1.808334832
C	0.518513518	2.279760048	-1.073787129
C	1.313534541	2.077815433	0.097769255
C	1.788721991	0.727134525	0.081458661
C	1.280172089	0.076520348	-1.093947008
H	-0.025633609	0.871688046	-2.736292143
H	0.003305454	3.192599802	-1.346573055
H	1.507435134	2.810539252	0.871626892
H	2.403868923	0.267929101	0.846086545
H	2.547069115	-1.326266875	-2.058041184
C	-0.939818298	0.259429741	1.919102275
C	-1.019156131	-0.864536234	1.027545705
C	-1.872523541	-0.474412927	-0.060102424
C	-2.29311848	0.877888686	0.151540721
C	-1.715738084	1.332348772	1.378538791
H	-0.359759682	0.290948244	2.834391211
H	0.393558928	-2.112096425	2.027067829
H	-2.132085356	-1.086857878	-0.915363122
H	-2.922408538	1.458949281	-0.511545828
H	-1.830010865	2.318601326	1.811394345
C	-0.389011812	-2.215677778	1.261888417
H	-1.155684414	-2.871044257	1.704029519
H	2.205553049	-2.137534762	0.360920974
C	0.207056277	-2.940208777	0.034442087
H	0.330134378	-3.993160766	0.322696412
H	-0.521267201	-2.944103119	-0.789738978
C	1.576884203	-2.44211535	-0.488640576
H	2.088400765	-3.304055043	-0.938485165
H	0.836032625	-1.597076022	-2.340159581
C	1.564324382	-1.330103476	-1.56108031

Table XI: Coordinates of the 2nd Minimum Structure

Transition 1 with no methyls			
Fe	0.787966208	-0.029834688	0.008611214
C	0.46548455	-1.773966442	-0.99659395
C	1.803936909	-1.732755717	-0.491985282
C	1.732976972	-1.594379377	0.930692014
C	0.350086101	-1.554307567	1.298016051
C	-0.445180685	-1.654905515	0.108038574
H	0.182494304	-1.861801118	-2.039422754
H	2.709769397	-1.784001736	-1.083662243
H	2.575553731	-1.521267234	1.607299887
H	-0.03919562	-1.442814265	2.303525081
H	-2.370264264	-1.768632825	1.031954765
C	0.675327834	1.728333621	1.039168076
C	-0.423595471	1.617390942	0.117902624
C	0.150119023	1.495254443	-1.194231937
C	1.57688	1.513520464	-1.075966594
C	1.902525149	1.659616663	0.309314417
H	0.577146733	1.832419961	2.113820704
H	-1.908386303	1.993174812	1.570943995
H	-0.401159744	1.39720598	-2.121892023
H	2.283582528	1.420012514	-1.891501847
H	2.899471421	1.694955787	0.731149421
C	-1.877258111	1.80656753	0.490362135
H	-2.193446999	2.752210985	0.027576666
H	-3.586242188	-0.874105533	-1.111600035
C	-2.962089793	0.723113138	0.155455556
H	-3.37180149	0.343996697	1.102304893
H	-3.796741499	1.246490895	-0.328406593
C	-2.628090313	-0.508087288	-0.717349252
H	-2.029375146	-0.22485718	-1.59168631
H	-2.232458426	-2.624773976	-0.492875462
C	-1.952133111	-1.692480206	0.018607616

Table XII: Coordinates of the 1st Transition State

Transition 2 with no methyls			
Fe	0.784806775	0.078217301	0.003473811
C	-0.074130586	1.502875674	1.191810126
C	1.338396968	1.716008753	1.095175243
C	1.66239413	1.903957338	-0.285406078
C	0.448802038	1.803467946	-1.034033325
C	-0.638781958	1.544139042	-0.129288239
H	-0.62115233	1.331195782	2.111251834
H	2.038525513	1.720836122	1.92165226
H	2.651546524	2.074929294	-0.692152205
H	0.353949241	1.892094399	-2.110370184
H	-2.138342174	1.711619288	-1.605869439
C	0.579152278	-1.492908889	-1.287869631
C	-0.213126638	-1.700198729	-0.109739966
C	0.688173605	-1.692788729	1.008869021
C	2.016013724	-1.469577436	0.524415868
C	1.948744722	-1.343345596	-0.899545302
H	0.193797464	-1.436471885	-2.299471999
H	-2.090079986	-2.077046215	-1.062420006
H	0.403790585	-1.817574145	2.047544526
H	2.911149583	-1.396108734	1.129870334
H	2.783727057	-1.156399888	-1.563573518
C	-1.701984173	-1.943457624	-0.043086298
H	-1.859982511	-2.904866405	0.466915742
H	-3.370264695	-0.121092788	-1.154057442
C	-2.544940626	-0.862127658	0.678933149
H	-3.450169112	-1.355456913	1.059268887
H	-2.004453877	-0.499174215	1.561703921
C	-3.030443664	0.311215095	-0.202348298
H	-3.935917316	0.716197366	0.26754694
H	-2.548322895	2.426372323	-0.069496986
C	-2.098732692	1.532290279	-0.524329895

Table XIII: Coordinates of the 2nd Transtion State

Intermediate 1 with no methyls			
Fe	-0.798741896	0.085370981	0.011083412
C	-0.577132006	-1.698989164	0.974931798
C	-1.944326849	-1.512919338	0.596774666
C	-1.989905417	-1.358209037	-0.824969506
C	-0.649240623	-1.45586327	-1.318595033
C	0.238846175	-1.656223932	-0.209253087
H	-0.217163714	-1.833400638	1.988291699
H	-2.792309178	-1.482968034	1.269898128
H	-2.8781304	-1.188474963	-1.42089531
H	-0.346020332	-1.362071944	-2.355157582
H	2.092725523	-1.642872581	-1.289193832
C	-0.496129012	1.789059862	-1.060699902
C	0.631603918	1.512279519	-0.212393059
C	0.145001399	1.506308183	1.138597286
C	-1.266082353	1.750895634	1.117933777
C	-1.662262556	1.930165048	-0.244770662
H	-0.465486529	1.849813938	-2.142568395
H	1.964624864	0.775844213	-1.690378869
H	0.736534237	1.31874747	2.026266248
H	-1.917632599	1.785542118	1.982425147
H	-2.667750737	2.123812629	-0.597602038
C	2.035764837	1.271061917	-0.711766669
H	2.516122318	2.241906231	-0.9094969
H	3.413589949	-1.445189906	1.074106287
C	2.986620008	0.464865511	0.200633821
H	3.916002122	0.321369598	-0.368718826
H	3.263305442	1.082780516	1.066768288
C	2.516294587	-0.912461645	0.73170164
H	1.896752075	-0.77200383	1.624975582
H	1.980320187	-2.868178114	-0.041570465
C	1.742915572	-1.817352989	-0.262344717

Table XIV: Coordinates of the 1st Intermediate Structure

Intermediate 2 with no methyls			
Fe	0.796561688	0.09621361	-0.031445161
C	0.165534944	-1.48774908	-1.160092904
C	1.595551627	-1.409002849	-1.17753072
C	2.058871185	-1.509897065	0.171972245
C	0.913498789	-1.643836872	1.017977175
C	-0.270284201	-1.618237293	0.201904554
H	-0.476904031	-1.428297412	-2.030022291
H	2.214447433	-1.286607724	-2.057899886
H	3.091402639	-1.476406873	0.497169447
H	0.926843615	-1.722235202	2.099061788
H	-1.693825366	-1.214917434	1.72327416
C	0.341219478	1.549566675	1.327393362
C	-0.598441244	1.558148322	0.242738668
C	0.155312792	1.79628191	-0.959335698
C	1.53902451	1.917378521	-0.616533424
C	1.656060524	1.760707384	0.800873442
H	0.094379557	1.378540977	2.369036863
H	-2.372893204	1.117510048	1.365496626
H	-0.252303254	1.85807363	-1.961621722
H	2.353824645	2.086006252	-1.309881794
H	2.575300619	1.787822909	1.372834402
C	-2.098397966	1.37688159	0.333711
H	-2.571175103	2.349777607	0.135500707
H	-3.732576971	-1.196454839	0.456085967
C	-2.675135358	0.331956608	-0.656559722
H	-3.677882944	0.653019827	-0.968996519
H	-2.063814401	0.343960088	-1.56631672
C	-2.810220393	-1.121448302	-0.137315354
H	-2.964361944	-1.776328836	-1.006754192
H	-1.924077377	-2.759196592	0.932360634
C	-1.67875932	-1.703386265	0.738838493

Table XV: Coordinates of the 2nd Intermediate Structure

Middle transition with no methyls			
Fe	0.809732561	0.078789663	-0.026142473
C	0.324807155	-1.587156	-1.096113204
C	1.745405833	-1.500361531	-0.940708772
C	2.035688332	-1.490973666	0.460351793
C	0.792140538	-1.572163405	1.164379639
C	-0.279774416	-1.618302281	0.207971565
H	-0.202866438	-1.596595081	-2.042330881
H	2.470064637	-1.443090988	-1.743599398
H	3.019282954	-1.423227894	0.908590762
H	0.670331871	-1.567646849	2.241549004
H	-1.915746347	-1.355096915	1.557555008
C	0.479915801	1.654691949	1.2192726
C	-0.584073365	1.526739026	0.261462657
C	0.01102822	1.656003635	-1.04094716
C	1.422424412	1.837900225	-0.883911086
C	1.713675635	1.8371144	0.516979995
H	0.36473417	1.590617386	2.295274092
H	-2.134871063	0.909557205	1.596062673
H	-0.511746752	1.596015349	-1.988028857
H	2.142011279	1.947667315	-1.685902108
H	2.693472493	1.944072554	0.965894514
C	-2.046074437	1.341278791	0.58985671
H	-2.510374974	2.337408867	0.654937147
H	-3.712284956	-1.476042422	-0.267356874
C	-2.871484173	0.515784429	-0.423118578
H	-3.927222243	0.745321752	-0.229564841
H	-2.673404485	0.912857976	-1.4267959
C	-2.72075047	-1.042019874	-0.449612381
H	-2.45349579	-1.359720393	-1.465443231
H	-2.013696227	-2.795920857	0.567646947
C	-1.74913485	-1.727653739	0.537672259

Table XVI: Coordinates of the Middle Transition State

Methylated minima 1			
Fe	0.265066723	-0.021572721	0.012539256
C	-0.234889466	-1.483686175	1.362619925
C	1.140370246	-1.097640761	1.53048779
C	1.173169031	0.309419917	1.827692611
C	-0.182203483	0.792224564	1.846627573
C	-1.055692992	-0.316544083	1.560870108
H	-0.022910727	-3.498652762	0.59397941
H	3.238278161	-1.509271383	1.185721515
H	2.28909453	2.163733424	1.885217491
H	0.138307546	2.932356024	1.94243497
H	-2.890456494	0.586763376	2.179503288
C	0.136151842	1.491715167	-1.367260868
C	-0.83973893	0.470621325	-1.650564487
C	-0.13343633	-0.766551683	-1.861577702
C	1.274197845	-0.508333775	-1.711902205
C	1.440832026	0.887838363	-1.408311637
H	-0.137562854	3.471730076	-2.174844486
H	-2.436897872	1.594412904	-2.495434318
H	-0.154479002	-2.931036743	-1.943137497
H	3.277281065	-1.260212606	-1.368809517
H	2.673225845	2.476615905	-0.602983567
C	-2.322106646	0.704495669	-1.858512933
H	-2.729853769	-0.129843723	-2.44549719
H	-4.417290351	-0.482993146	0.560938879
C	-3.213056283	0.890829479	-0.610071162
H	-2.849313444	1.740512106	-0.016354017
H	-4.209368143	1.184234533	-0.969183611
C	-3.357481803	-0.356713828	0.299129822
H	-3.081323809	-1.258410149	-0.264299215
H	-2.885218499	-1.161732215	2.243597499
C	-2.569259315	-0.306849818	1.627038434
C	2.397635929	1.112652481	2.175786107
H	2.585629997	1.088421807	3.258810095
H	3.294308623	0.726550231	1.678892646
C	-0.606623357	2.183884846	2.234352398
H	-1.554379006	2.468711779	1.765861829
H	-0.739544801	2.260956135	3.323235892
C	-0.736711503	-2.888623113	1.159125485
H	-0.898224217	-3.38767837	2.125786932
H	-1.686940601	-2.908907266	0.61584908

C	2.326608609	-2.023585861	1.509850277
H	2.519085749	-2.434082698	2.511443679
H	2.170587882	-2.870545155	0.832617839
C	2.380326328	-1.501111958	-1.949704073
H	2.077356012	-2.51852586	-1.677558871
H	2.669766224	-1.516591053	-3.010295811
C	2.75351658	1.610691026	-1.269358746
H	3.536017149	0.958586358	-0.865412031
H	3.102564152	1.977523053	-2.245238985
C	-0.149612331	2.960658158	-1.201067563
H	-1.130727279	3.137948892	-0.748878976
H	0.597154182	3.452094539	-0.567140095
C	-0.738267522	-2.074547091	-2.298052768
H	-1.759307262	-2.199298167	-1.922858628
H	-0.778964661	-2.137536197	-3.395163206

Table XVII: Coordinates of the 1st Minimum Structure

Methylated minima 2			
Fe	-0.266257476	0.000321105	-0.002608134
C	0.136103133	-1.770146015	0.961434667
C	-1.244039587	-1.720114044	0.557091342
C	-1.283370463	-1.561186464	-0.872098147
C	0.071846927	-1.510150174	-1.350465473
C	0.952485761	-1.641737816	-0.218088353
H	-0.061804734	-1.649055676	3.114807107
H	-3.324656281	-1.410587168	1.074992156
H	-2.382132998	-0.975551904	-2.643783203
H	-0.211991349	-0.903973118	-3.412095512
C	0.153071554	1.770985913	-0.958755033
C	0.952208082	1.639923394	0.232505863
C	0.054977071	1.508431987	1.351663914
C	-1.293123371	1.562951392	0.853665162
C	-1.232825232	1.723185635	-0.574500475
H	0.756746266	3.124897341	-2.524961291
H	-0.261351705	0.902726751	3.408716116
H	-3.400144434	1.156357222	1.148307166
H	-2.207759914	1.543530457	-2.499556672
C	2.457051149	1.789162787	0.322146621
C	3.300525327	0.523246874	0.592347706
C	3.306900585	-0.528779276	-0.546499914
C	2.458223805	-1.793257908	-0.286194413
H	2.820332744	2.245818491	-0.608538255
H	2.676768086	2.522247099	1.112932837
H	4.331831653	0.858287061	0.770630716
H	2.975599928	0.050429667	1.529217372
H	2.99442238	-0.055386283	-1.487243185
H	4.339963982	-0.865107384	-0.71172475
H	2.688254757	-2.528216187	-1.072275051
H	2.807810959	-2.24815757	0.650571107
C	-2.520464704	-1.562567026	-1.729072114
H	-2.784755882	-2.586019337	-2.031562914
H	-3.383585019	-1.144300483	-1.199231706
C	0.492640171	-1.473928902	-2.795774768
H	1.480388063	-1.019634458	-2.922384593
H	0.54122202	-2.490850845	-3.211762962
C	0.626279104	-2.043211093	2.35875221
H	0.72087427	-3.124710205	2.533849957
H	1.60655825	-1.592170628	2.544935739

C	-2.4334618	-1.919828079	1.457605571
H	-2.67869556	-2.987643152	1.549443663
H	-2.246738851	-1.538189335	2.467715697
C	-2.542269786	1.566244616	1.692998064
H	-2.420553713	0.972938251	2.605984103
H	-2.804821039	2.589378649	1.998031354
C	-2.408508607	1.925590409	-1.492297159
H	-3.306391472	1.41834775	-1.122934392
H	-2.650081326	2.99394562	-1.587628089
C	0.663555301	2.043425875	-2.348941961
H	1.648124022	1.595496926	-2.519215903
H	-0.011399058	1.645055511	-3.11460605
C	0.45421393	1.470433084	2.803019063
H	1.438423679	1.012588121	2.944078469
H	0.500126548	2.487109077	3.219848205

Table XVIII: Coordinates of the 2nd Minimum Structure

Methylated transition 1			
Fe	-0.279123309	-0.014599587	-0.032783532
C	-0.051095492	-1.800972731	0.948364989
C	-1.360674936	-1.716420085	0.359653294
C	-1.200339044	-1.538105377	-1.059399871
C	0.209261714	-1.511693219	-1.347519048
C	0.922090628	-1.663845181	-0.10681265
H	-0.476687059	-1.601172312	3.064373667
H	-3.481138067	-1.347573646	0.59482536
H	-2.03117329	-0.894317612	-2.951942658
H	0.193381254	-0.883987021	-3.41922657
C	-0.09420317	1.741308951	-1.057206072
C	0.963590858	1.604229839	-0.079364413
C	0.344882121	1.515938963	1.218062877
C	-1.08048331	1.549897279	1.03853283
C	-1.353898951	1.704924618	-0.363468046
H	0.127173312	3.062568693	-2.7495669
H	0.840371052	0.672704655	3.175972841
H	-3.050822468	1.12054177	1.830017366
H	-2.751445179	1.550895737	-2.014412299
C	2.438932217	1.732615819	-0.396799864
C	3.499730144	0.6668454	0.06487349
C	3.114913067	-0.612198226	0.841293487
C	2.423143943	-1.753353152	0.057838197
H	2.522869996	1.830747379	-1.484724986
H	2.764922603	2.707992549	-0.004822599
H	4.064139081	0.349266536	-0.82402631
H	4.232776464	1.192521524	0.691566877
H	4.062507388	-1.015795215	1.227702718
H	2.517968605	-0.358471764	1.721444551
H	2.894318443	-1.843485809	-0.930293812
H	2.646790949	-2.699186305	0.57451036
C	-2.309794241	-1.490615501	-2.07532768
H	-2.5591108	-2.500399972	-2.431728211
H	-3.223515579	-1.054336128	-1.657560317
C	0.826034555	-1.43928559	-2.718825572
H	1.804972899	-0.947111761	-2.700361325
H	0.970743447	-2.446695533	-3.134940327
C	0.229207078	-2.108886231	2.39593652
H	0.138047991	-3.188048882	2.586543071
H	1.239456031	-1.811084254	2.69329289

C	-2.666311397	-1.889741923	1.088346491
H	-2.956066098	-2.949690301	1.129608522
H	-2.60632755	-1.525387296	2.119898211
C	-2.093306131	1.544248899	2.152196936
H	-1.744347915	0.956125145	3.009217482
H	-2.289230108	2.564883457	2.512288893
C	-2.714734863	1.90060876	-0.977097865
H	-3.491646371	1.362460856	-0.42125207
H	-2.992295284	2.964547274	-0.979359368
C	0.072851743	1.985759503	-2.534020007
H	0.983103919	1.524037545	-2.930576268
H	-0.770836702	1.580913186	-3.104940226
C	1.029173171	1.562715728	2.562506607
H	2.112880445	1.671804474	2.456651525
H	0.671606418	2.430463034	3.133603961

Table XIX: Coordinates of the 1st Transition State

Methylated intermediate 1			
Fe	0.169588749	-0.05407734	-0.228733908
C	-0.959912007	-1.774580637	-0.198154174
C	0.164662791	-1.926521171	-1.081033293
C	1.36470299	-1.724099513	-0.31576947
C	0.982451984	-1.443622017	1.043356509
C	-0.456583244	-1.455732663	1.117686492
H	-2.668153805	-1.538657992	-1.521457555
H	0.947526166	-1.957044357	-3.099503792
H	3.480799407	-1.259990273	-0.270218393
H	2.890289154	-0.852979828	1.876552468
C	1.134264075	1.697390107	0.180232654
C	-0.230932482	1.727314427	0.662465099
C	-1.09558528	1.568292744	-0.481013613
C	-0.26764793	1.380626888	-1.642501786
C	1.107212091	1.47494596	-1.239687554
H	2.617489378	3.038133714	0.982445155
H	-3.088619578	0.831485957	-0.982997207
H	-0.064690023	0.695241529	-3.685978683
H	3.195656197	1.071626688	-1.657791437
C	-0.561058452	1.900500928	2.132426513
C	-1.870039459	1.316563665	2.723291995
C	-2.328580711	-0.103199793	2.321673407
C	-1.283791539	-1.24763794	2.37198486
H	0.276449883	1.465649487	2.693287537
H	-0.545728729	2.973610939	2.38291274
H	-1.749261217	1.346888889	3.816392564
H	-2.703936374	1.999786299	2.50990458
H	-3.15527237	-0.363277341	2.998518881
H	-2.764111014	-0.070348062	1.320071028
H	-0.614931907	-1.095715097	3.229618814
H	-1.817580266	-2.186584248	2.583511953
C	2.772108364	-1.88638138	-0.824029575
H	3.108424358	-2.928324205	-0.722660721
H	2.853542351	-1.616904222	-1.882720921
C	1.933440533	-1.277216922	2.198561418
H	1.529233584	-0.620196359	2.97705248
H	2.145840948	-2.248520116	2.66777381
C	-2.387077425	-2.056526677	-0.595506207
H	-2.525763147	-3.132567058	-0.772689888
H	-3.100930519	-1.762533856	0.178579664

C	0.091676362	-2.334730796	-2.528275481
H	0.087991636	-3.429898092	-2.629414725
H	-0.817778586	-1.957849216	-3.009636148
C	-0.776397125	1.235279364	-3.051980163
H	-1.726548067	0.689405266	-3.084942747
H	-0.947497673	2.218954707	-3.513656298
C	2.29859053	1.450343595	-2.159292565
H	2.119179029	0.815456607	-3.034575498
H	2.529249835	2.459902496	-2.528864964
C	2.377029879	1.965175362	0.988230336
H	2.268175482	1.662316941	2.034441593
H	3.246019421	1.434104999	0.582386409
C	-2.595751125	1.719226507	-0.567183583
H	-3.047595388	1.92934675	0.403855236
H	-2.843472555	2.563029653	-1.226005248

Table XX: Coordinates of the 1st Intermediate Structure

Methylated midtransition			
Fe	0.306700998	0.020097142	-0.014326945
C	-0.274393927	-1.656457975	-1.049341862
C	1.162551513	-1.602248448	-0.948902802
C	1.516700372	-1.582413399	0.443279947
C	0.301015363	-1.617617445	1.209037439
C	-0.815659891	-1.638738907	0.291276594
H	-0.361362609	-1.688446262	-3.205538048
H	3.081160647	-1.166975543	-1.844302246
H	2.975899485	-1.106448558	1.969970678
H	1.083240382	-1.24341058	3.191969848
C	0.089483935	1.617192111	1.242963139
C	-1.020475886	1.51352703	0.322601169
C	-0.485646425	1.629011448	-1.015760575
C	0.946256048	1.758617263	-0.912273974
C	1.299709004	1.755302265	0.480208578
H	-0.117774733	2.734555435	3.071942838
H	-0.576578433	1.680450253	-3.17160658
H	2.90494568	1.592938999	-1.811458078
H	2.807959506	1.438870563	2.000610426
C	-2.462719026	1.407563138	0.775382366
C	-3.471363809	0.559002552	-0.035300732
C	-3.369600366	-1.003203391	-0.049865808
C	-2.2583041	-1.728394675	0.746124452
H	-2.469580754	1.05408951	1.814719299
H	-2.879299392	2.427446239	0.819008696
H	-4.458889207	0.816680174	0.370839658
H	-3.493258065	0.924986851	-1.066461038
H	-4.314891161	-1.394292455	0.350152079
H	-3.344794369	-1.349715416	-1.087656166
H	-2.30844278	-1.39696558	1.791531873
H	-2.539400222	-2.794203094	0.771604348
C	2.913592531	-1.618214525	1.003232573
H	3.25061343	-2.653518879	1.15598483
H	3.631695503	-1.134248554	0.331890101
C	0.231590367	-1.734480053	2.708733463
H	-0.67841903	-1.288071644	3.122709189
H	0.24507673	-2.790686911	3.013817142
C	-1.021575024	-1.843865747	-2.346049897
H	-1.414895656	-2.867713038	-2.41832532
H	-1.867510757	-1.161319964	-2.463626041

C	2.135706761	-1.659720104	-2.096867159
H	2.368580745	-2.699618651	-2.367450354
H	1.744327817	-1.165459145	-2.992812138
C	1.903976042	1.965409459	-2.056005168
H	1.579294529	1.444459563	-2.963411027
H	2.001197727	3.032206124	-2.303656577
C	2.680201437	1.959089058	1.044873807
H	3.454861337	1.586573057	0.365376639
H	2.880622333	3.025703167	1.220762115
C	0.005305666	1.692196047	2.744581801
H	-0.839503703	1.123279306	3.146361323
H	0.913121752	1.304958517	3.219837741
C	-1.249926941	1.745687102	-2.310694263
H	-2.010232005	0.970565548	-2.438513158
H	-1.760532551	2.717348465	-2.369170023

Table XXI: Coordinates of the Middle Transition State

References

1) Kealy, T.J.; Pauson, P.L. *Nature* **1951***, 168*, 1039.

2) Miller, S.A.; Tebboth, J.A.; Tremaine, J.F. *J. Chem. Soc.* **1952**, 632.

3) Yamamoto, A. *Organotransition Metal Chemistry*; Wiley, 1986, p. 184.

4) Wilkinson, G.; Rosenblum, M.; Whitting, M.C.; Woodward, R.B. *J. Am. Chem. Soc.* **1952**, *74*, 2125.

5) Woodward, R.B.; Rosenblum, M.; Whitting, M.C. *J. Am. Chem. Soc.* **1952***, 74*, 3458

6) Fischer, E.O.; Pleszke, K. *Chem. Ber.* **1958**, *91*, 2719.

7) a) Eiland, P.F.; Pepinsky, R. *J. Am. Chem. Soc.* **1952***, 74*, 4971. b) Dunitz, J.C.; Orgel, L.E. *Nature* **1953***, 171*, 121

8) Haaland, A. *Acc. Chem. Res.* **1979***, 12*, 415.

9) Lauher, J.W.; Hoffmann, R. *J. Am. Chem. Soc.* **1976***, 98*, 1729.

10) Shriver, D.; Atkins, P. *Inorganic Chemistry;* Freeman, **1999**, pp.566-8

11) Mueller-Westerhoff, U.T. *Angew. Chem. Int. Ed. Engl.* **1986***, 25*, 702.

12) Lüttringhaus, A.; Kullick, W. *Angew. Chem.* **1958**, *70*, 438.

13) Hisatome, M.; Watanbe, J.; Kawajiri, Y.; Yamakawa, K. *Organometallics* **1990,** *9*, 497.

14) Hillman, M.; Fujita, E.; Dauplaise, H. *Organometallics* **1984***, 3,* 1170.

15) It is unknown if this occurs in the single tether ferrocene because no crystal has been taken of it.

16) Singletary, N.J.; Hillman, M.; Dauplaise, H.; Kvick, A.; Kerber, R. C. *Organometallics,* **1984***, 3*, 1427.

17) Itoh, K.; Kinoshita, M. *Molecular magnetism*, Kodansha LTD. 2000.

18) Orchard, A.F. *Magnetochemistry*, Oxford University Press. 2003.

19) Carlin, R.L. *Magentochemistry*, Springer-Verlag. 1986.

20) Miller, J.S.; Calabrese, J.C.; Rommelmann, H.; Chittipeddi, S.K.; Zhang, J.H.; Reiff, W.M.; Epstein, A.J. *J. Am. Chem. Soc.* **1987**, *109*, 769.

21) Miller, J.S.; Glatzhofer, D.T.; O'Hare, D.M.; Reiff, W.M.; Chakraborty, A.; Epstein, A.J. *Inorg. Chem.* **1989***, 28*, 2930.

22) Harris, D.T.; Castellani, M.P.; Rheingold, A.L.; Reiff, W.M.; Yee, G.T. *Inorg. Chim. Acta* **2006***, 359*, 4651.

23) This is not an original synthesis, but no literature report on its isolation was found.

24) Threlkel, R. S.; Bercaw, J. E.; Seidler, P. F. *Org. Synth*. **1987**, *65*, 42.

25) Robbins, J.L.; Edelstein, N.; Spencer, B.; Smart, J.C. *J. Am. Chem. Soc.* **1982**, *104*, 1882.

26) Tobita, H.; Habazaki, H.; Shimoi, M.; Ogino, H. *Chem. Lett.* **1988**, 1041.

27) Hisatome, M.; Kawaziri, Y.; Yamakawa, K. *Tetrahedron Lett.* **1979**, *20*, 1777.